Anaerobic microbial defluorination of polyfluoroalkylether substances (ether PFAS): Transformation pathways and roles of different microorganisms

Bosen Jin[1], Weiyang Zhao[1], Yiwen Zhu[1], Zekun Liu[1], Yaochun Yu[1], Shun Che[1], Jinyong Liu[1], and Yujie Men[1*]

[1]Department of Chemical and Environmental Engineering, University of California, Riverside, California, 92521, United States

***Corresponding Author**

Yujie Men

Department of Chemical and Environmental Engineering

University of California, Riverside

Address: A235 Bourns Hall, 3401 Watkins Drive, Riverside, CA 92521

Email: ymen@engr.ucr.edu

Phone: (951) 827-1019

Abstract

Polyfluoroalkylether substances (ether PFAS) are widely detected in the environment, but knowledge of their environmental fate through biological processes remains limited. This study reports the microbial transformation of environmentally relevant ether PFAS and key microbial groups involved in the anaerobic biotransformation process. The investigated ether PFAS include mono- and dichlorinated ones such as 6:2 chlorinated polyfluorooctane ether sulfonate (F53-B) and 6,7-dichloroperfluoro-5-oxaheptanoic acid, as well as unsaturated ones such as sodium *p*-perfluorous nonenoxybenzenesulfonate (OBS), Nafion Byproduct 1 (NBP1) and its analogues. The presence of chlorine-substitution and unsaturated carbon facilitated the biotransformation and defluorination of ether PFAS. For fully halogenated ether PFAS, biotransformation only occurred under anaerobic conditions via dechlorination (reductive, eliminative, and hydrolytic), hydrolytic O-dealkylation, and reductive defluorination, forming less fluorinated and shorter-chain products. Strong evidence from community and pure culture experiments indicated the involvement of cobalt-enzyme-dependent microorganisms, such as *Sporomusa sphaeroides*, in the initial dechlorination step during the biotransformation of chlorinated ether PFAS. Meanwhile, microorganisms independent of cobalt-enzymes, such as *Desulfovibrio aminophilus*, were responsible for the biotransformation of non-chlorinated unsaturated ether PFAS (e.g., NBP1), especially for the hydrolytic O-dealkylation reaction. The findings provide significant insights into the fate of ether PFAS in anaerobic environments and underscore the cooperation of different microbial groups in a community to achieve further transformation and higher defluorination.

Keywords: ether PFAS, defluorination, dechlorination, cobalt enzymes, *Sporomusa sphaeroides*, *Desulfovibrio aminophilus*

Synopsis: This study uncovers the biotransformation and defluorination mechanisms of environmentally relevant ether PFAS and identifies key anaerobic microbial groups driving these processes.

TOC art:

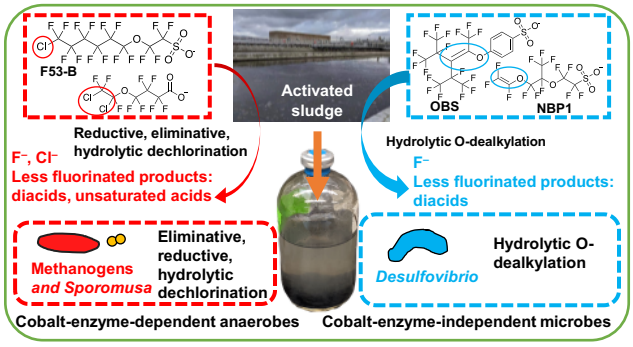

Introduction

Per- and polyfluoroalkyl substances (PFAS) consist of a large group of persistent organic pollutants due to the presence of many strong carbon–fluorine (C–F) bonds.[1] Although these anthropogenic organofluorines have been discharged into the environment for decades, microorganisms have not evolved effective pathways to degrade them.[2] These compounds, especially the fully fluorinated and long-chain PFAS, are not only notoriously persistent but also toxic,[1, 3] accumulating in biological systems across plants, animals, and humans.[4-8] As a result, the U.S. Environmental Protection Agency (USEPA) has established maximum contaminant levels (MCLs) for six PFAS in drinking water.[9] Besides five legacy perfluoroalkyl acids (PFAAs), the list also includes hexafluoropropylene oxide dimer acid and its ammonium salt (a.k.a. GenX) in the ether PFAS category.

Ether PFAS are manufactured for various applications and have recently gained increasing attention.[1, 10-13] The USEPA-regulated GenX has been used as an alternative to PFOA.[10] Other ether PFAS, such as 6:2 and 8:2 chlorinated polyfluorooctane ether sulfonate (6:2 and 8:2 Cl-PFESA, a.k.a. F-53B)[12, 14] and sodium *p*-perfluorous nonenoxybenzene sulfonate (OBS)[15, 16] were developed as PFOS replacements. Some ether PFAS are used in fluoropolymer manufacturing as building blocks, such as Nafion byproducts (NBPs).[11, 17] Nafion is a perfluoroether sulfonic acid polymer with essential applications in the chlor-alkali process, analytical devices, energy storage and production.[17-21] Although ether PFAS alternatives like GenX and F-53B were initially invented with the expectation of being less bioaccumulative and hence less toxic,[13] studies reported their toxicities to human health and ecosystems via mode of action similar to the legacy PFAS.[22-28] The regulation of GenX and the increasingly documented toxicities of other ether PFAS underscore the need for a more comprehensive understanding of

81 the environmental fate, transport, and degradation of ether PFAS in use, providing guidance for
82 risk assessment and mitigation.

83 Ether PFAS have been detected in diverse environmental matrices, including those
84 alternatives to PFOA/PFOS[29-31] and NBPs involved in fluoropolymer manufacturing[32-36],
85 suggesting their persistence in the environment. Although perfluoroalkyl ether acids are resistant
86 to environmental degradation (e.g., biological degradation and chemical oxidation by radicals),
87 polyfluoroalkyl ether acids have exhibited aerobic microbial transformation activities.[37] Our
88 previous study revealed that the presence of ether groups (–O–) together with non-fluorinated
89 carbon (e.g., $–CH_2–$) enhanced the biodegradability of polyfluoroalkyl ether acids. Other
90 microbially amenable moieties in PFAS compounds leading to significant transformation and
91 defluorination have also been identified, including Cl-substitutions for anaerobic defluorination
92 and C═C double bonds for both aerobic and anaerobic defluorination. The presence of those
93 moieties together with ether groups suggests the biotransformation potential of specific ether
94 PFAS, but studies on those structures are scarce. There are only reports on F-53B (6:2 and 8:2
95 Cl-PFESA) undergoing partial biotransformation via reductive dechlorination forming H-PFESA
96 without defluorination,[38, 39] with the environmental fate of other ether PFAS with Cl-substitutions
97 and/or C═C bonds (e.g., OBS and NBPs) remaining unknown.

98 Thus, in this study, we aimed to elucidate the biotransformation potential and pathways
99 of environmentally relevant ether PFAS with Cl-substitutions and C═C bonds in anaerobic
100 microbial communities and identify responsible microbial groups. Five representative
101 chlorinated or unsaturated ether PFAS were selected, whose biotransformability was investigated
102 in both anaerobic and aerobic conditions. Biotransformation and defluorination pathways were
103 elucidated based on the parent compound decay and the formation of fluoride ion and

transformation products. Major biotransformation reactions and key microbial groups involved were identified. These findings advance the understanding of the environmental fate of ether PFAS, providing critical insights into risk assessment, source tracking, and the design of more readily biodegradable alternatives.

Materials and Methods

PFAS chemicals

In this study, we investigated four ether PFAS (**Table 1**), including two chlorinated ether PFAS (i.e., one major component in F-53B, 6:2 Cl-PFESA and a dichlorinated perfluorocarboxylic acid, **Cl-E1** and **Cl-E2**) and three unsaturated ether PFAS (i.e., OBS, NBP1, and an NBP1 analogue, denoted "**E1**", "**E2**", and "**E3**", respectively). Additionally, the available reference compounds of identified plausible transformation products (TPs) of the parent compounds were obtained (**Table 1**) for the structural confirmation and quantification of TPs.

Table 1. List of the investigated ether PFAS and select TPs and analytical properties

Ether PFAS and TPs	ID #	CAS #	Structure and formula	Purity (%)	RT (min)	LOD (nM)	LOQ (nM)
Potassium;2-(6-chloro-1,1,2,2,3,3,4,4,5,5,6,6-dodecafluorohexoxy)-1,1,2,2-tetrafluoroethanesulfonate[1]	Cl-E1 (F-53B, major)	73606-19-6	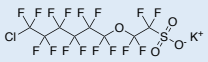 $C_8ClF_{16}KO_4S$	≥96	7.61	5	10
4-(1,2-dichloro-1,2,2-trifluoroethoxy)-2,2,3,3,4,4-hexafluorobutanoic acid[2]	Cl-E2	86556-81-2	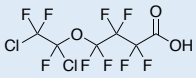 $C_6HCl_2F_9O_3$	97	6.93	10	30
Sodium;4-[1,1,1,4,5,5,5-heptafluoro-3-(1,1,1,2,3,3,3-heptafluoropropan-2-yl)-4-(trifluoromethyl)pent-2-en-2-yl]oxybenzenesulfonate[1]	E1 (OBS)	70829-87-7	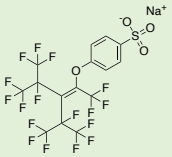 $C_{15}H_4F_{17}NaO_4S$	≥96	7.81	5	10

1,1,2,2-tetrafluoro-2-[1,1,1,2,3,3-hexafluoro-3-(1,2,2-trifluoroethenoxy)propan-2-yl]oxyethanesulfonic acid[(2)]	E2 (NBP1)	29311-67-9	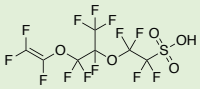 $C_7HF_{13}O_5S$	95	7.18	10	30
1,1,2,2-Tetrafluoro-2-(1,2,2-trifluorovinyloxy)ethanesulfonic acid**	E3	111173-24-1	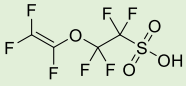 $C_4HF_7O_4S$	97	6.02	5	10
2,2,3,3-tetrafluorosuccinic acid[(2)]	TP188_Cl-E2	377-38-8	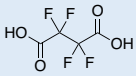 $C_4H_2F_4O_4$	98	0.87	5	10
2-chloro-2,2-difluoroacetic acid[(2)]	TP128_Cl-E2	189539-2	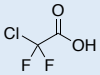 $C_2HClF_2O_2$	97	1.38	50	100
2,2-difluoro-2-sulfoacetic acid[(3)]	TP174_E2/E3	422-67-3	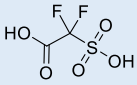 $C_2H_2F_2O_5S$	>98	0.86	10	30

*: Reference compounds of ether PFAS and their TPs were obtained from (1) Dr. Jinyong Liu's Lab (Riverside, CA, USA), detailed information can be found from their previous study,[40] (2) SynQuest Laboratories, Inc. (Alachua, FL, USA), and (3) Santa Cruz Biotechnology, Inc. (Dallas, TX, USA).
**: This compound is derived from the hydrolysis of 1,1,2,2-tetrafluoro-2-((1,2,2 trifluoroethenyl)oxy)ethanesulfonyl fluoride (CAS No. 29514-94-1) ordered from SynQuest Laboratories, Inc.

Biotransformation of ether PFAS

Anaerobic biotransformation batch reactors were set up in 160-mL sealed serum bottles according to a previous study,[41] using fresh settled activated sludge (6700–6800 mg total suspended solids/L) from a local municipal wastewater treatment plant. Each bottle contained 90 mL autoclaved basal medium including 100 μg/L vitamin B_{12} and other vitamins (the recipe was the same as reported previously[41]) and 10 mL settled sludge, with a headspace of Ar/CO_2 (75:25, v/v). Ether PFAS was spiked into the culture (50 – 100 μM initial concentrations), and methanol (~123 mM) was added as the electron donor and re-added bi-weekly. The pH was maintained at 7.4 ± 0.1. Biomass-free abiotic control and heat-inactivated biomass control were prepared using the same medium, with autoclaved sludge filtrate (0.22 μm) and autoclaved sludge, respectively, replacing the settled activated sludge. Sodium azide (~ 0.2 g/L) was added to these controls to

136 prevent cell growth and activity during incubation. All cultures, including biotransformation
137 groups and controls, were incubated in the dark at 34 °C without shaking. Triplicates were
138 included in all conditions. A sludge-only control was also set up to account for the sludge matrix
139 background for TP analysis. Aerobic biotransformation experiments were also set up using the
140 activated sludge taken from the same plant using the previously reported procedure (also see
141 Supplemental Methods in the SI).[37]

142 For all transformation groups (i.e., anaerobic, aerobic, and abiotic controls), 2-mL
143 samples were taken over a time course and centrifuged at 16,000 × g, 4 °C for 35 minutes. The
144 supernatant was collected to measure fluoride, the parent compound, and TPs. Cell pellets were
145 extracted with 1 mL methanol containing 0.1% NH_4OH, and ^{13}C-labeled PFOA was added as the
146 extraction surrogate to account for extraction recoveries. Cell samples were vortexed and
147 ultrasonicated for 30 minutes. The cell extract was then collected by centrifugation (16,000 × g,
148 4 °C for 35 minutes). Parent compounds and TPs detected in the cell extract represent the
149 biomass-associated fraction, either through passive adsorption or active cellular uptake. Both **Cl-**
150 **E1** and **E1** exhibited significant bioadsorption (> 20%), but not for the other compounds (**Figure**
151 **S1**). Here, the total concentration of the parent compounds and TPs, i.e., the sum of extracellular
152 and cell-associated concentrations, was presented in all figures and used to elucidate
153 biotransformation pathways.

154 **The role of cobalt-enzyme-dependent microorganisms in anaerobic biotransformation of**
155 **ether PFAS**

156 The anaerobic community was incubated under two distinct conditions, each in triplicates. The
157 cultures were set up using freshly taken activated sludge: one in the normal basal medium with
158 vitamin B_{12} and the other in the same basal medium but without cobalt ion or v

159 itamin B_{12}. The chlorinated ether PFAS, **Cl-E2**, and the non-chlorinated, unsaturated ether PFAS
160 **E2** were spiked separately for comparison. Fluoride ions, parent compounds, and TPs were
161 analyzed over a time course of ~ 130 days.

162 **The role of methanogens in the anaerobic biotransformation of Cl-E2**

163 Methanogen inhibition experiments were conducted to examine the role of methanogens in the
164 biotransformation of **Cl-E2** in the anaerobic microbial community. Methanogens in the anaerobic
165 community were inhibited by the addition of 0.5 mM 2-bromoethanesulfonate (BES), a known
166 inhibitor of methanogenesis.[42] Biotransformation activities, in terms of fluoride formation, parent
167 compound degradation, and TP formation, were compared to the no-BES control. All conditions
168 were performed in triplicate.

169 **Anaerobic biotransformation by pure cultures**

170 Biotransformation of the ether PFAS was further investigated using two anaerobic pure cultures,
171 *Sporomusa sphaeroides* (DSM 2875) and *Desulfovibrio aminophilus* (DSM 12254), previously
172 shown to carry out anaerobic biotransformation of chlorinated PFAS.[41] The two pure cultures
173 were obtained from the DSMZ-German Collection of Microorganisms and Cell Cultures GmbH
174 (Braunschweig, Germany). Both cultures were grown in the basal medium used for the anaerobic
175 biotransformation experiments, supplemented with 10 mM sodium lactate as the electron donor.
176 For the sulfate-reducing *D. aminophilus*, 2 mM of sodium sulfate was also added. To assess the
177 biotransformation of **Cl-E2** and **E2**, each culture was inoculated (10% v/v) into 45 mL of fresh
178 medium containing 50 μM of individual ether PFAS. Samples (2 mL) were periodically collected
179 during the incubation for fluoride, parent compound, and TP analyses. Cell densities were
180 determined by genomic DNA quantification (see Supplemental Methods in the SI).

181 **Fluoride Measurement**

182 The HQ30D Portable Multi Meter (HACH), coupled with an ion-selective electrode (ISE,
183 HACH), was utilized for fluoride ion (F^-) measurement, with a limit of quantification (LOQ) of
184 0.02 mg/L (~1 μM). The fluoride measurement accuracy within the same matrix was validated
185 using ion chromatography in our previous studies.[41, 43] The defluorination degree (Def %) was
186 determined using the equation:

187 $$\text{Defluorination degree (\%)} = \frac{\text{F}^- \text{ formation } (\mu\text{M})}{\text{Removed conc. (uM)} \times \text{\# of F in one molecule}} \times 100\%$$

188

189 **Ultra-High-Performance Liquid Chromatography Coupled to High-Resolution tandem**
190 **Mass Spectrometry (UHPLC-HRMS/MS) Analysis**

191 Ether PFAS were analyzed using a UHPLC-HRMS/MS system (Q Exactive, Thermo Fisher
192 Scientific, Waltham, MA). For the UHPLC, a 2-μL sample was loaded onto a Hypersil Gold
193 column (particle size 1.9 μm, 2.1×100 mm, Thermo Fisher Scientific). The loaded sample was
194 eluted using a UHPLC mobile phase consisting of (A) 10 mM ammonium acetate in Milli-Q
195 water and (B) 10 mM ammonium acetate in HPLC grade methanol, at 300 μL/min with a linear
196 gradient: 95% A (0 – 1 min), 95–5% A (1 – 6 min), 5% A (6 – 8.75 min), and 95% A (8.75 – 12.5
197 min). For HRMS, negative electrospray ionization (ESI^-) was used, with a full MS scan (m/z 70
198 – 1050) at a resolution of 70,000 @ m/z 200 and a data-dependent MS^2 scan (dd-MS2) at a
199 resolution of 17,500 @ m/z 200, at a normalized collision energy (NCE) of 25. Peak areas for
200 parent compounds and TPs were quantified using TraceFinder 4.1 EFS and Freestyle 1.8
201 (Thermo Fisher Scientific). Concentrations of parent compounds and TPs were determined using
202 matrix-matched calibration standard series.

203 **TP identification and biotransformation pathway elucidation**

Suspect screening was performed using TraceFinder 4.1 EFS against a custom-compiled list of potential TPs from different anaerobic biotransformation pathways such as reductive, eliminative, and hydrolytic dechlorination, reductive defluorination, HF elimination, O-dealkylation, etc. Non-target screening was done using the "Expected and Unknown Met ID (Metabolite Identification) Workflow" in Compound Discover 3.3 (Thermo Fisher Scientific). The criteria used for identifying plausible TPs were: (1) ≤ 5 ppm mass tolerance; (2) proper peak shape with peak areas > 10^5; (3) isotopic pattern score > 70; (4) significant and discernible formation trend over time; (5) no detection in abiotic, heat-inactivated, or sludge-only matrix controls; and (6) exclusion of in-source fragments. TP structures were elucidated based on MS^2 fragmentation profiles. Structures of TPs with available reference compounds were further confirmed by comparing the retention time (RT), MS^1/MS^2 profiles between the TP and the reference standard. Confidence levels of TPs were assigned according to widely adopted criteria for general TP identification[44] and PFAS-specific non-target analyses.[45] The most plausible biotransformation pathways were then proposed based on: (1) parent compound removal, (2) fluoride formation trend, and (3) TP formation trend with confirmed formulas or structures. These trends should be correlated stoichiometrically or qualitatively. In other words, the parent compound decrease is followed by primary TP increase, the decrease of which leads to the formation of secondary TPs. Stable intermediates should remain as the end products, which will reach a plateau once their precursors are depleted. In addition, fluoride formation should be stoichiometrically reasonable according to the parent compound removal and lead to the formation of less-fluorinated TPs.

Results and Discussion

Anaerobic biotransformation and defluorination of Cl-E1 (F-53B major) and Cl-E2 by activated sludge communities

Cl-E1 and **Cl-E2** only exhibited substantial removal with F^- formation in the sludge community under anaerobic conditions (**Figure 1A&C**), whereas no transformation or defluorination was observed under aerobic conditions or the abiotic controls (**Figure S2A&B** and **Figure S3**). This is consistent with our previous findings that fully halogenated compounds like chlorofluorocarboxylates lacking carbon-hydrogen bonds are unlikely biotransformed in aerobic conditions.[41]

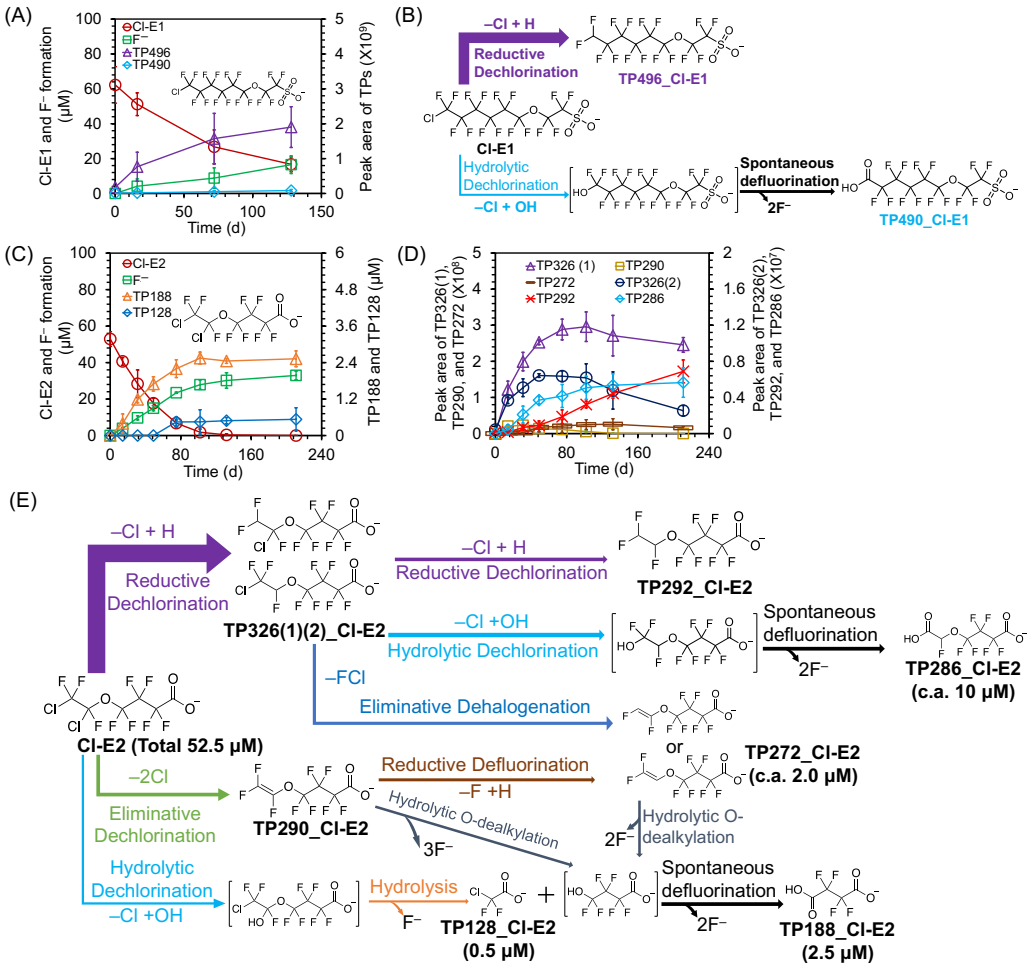

Figure 1. Biotransformation and defluorination of **Cl-E1** and **Cl-E2** under anaerobic conditions. (A) Parent compound decay of **Cl-E1**, F^- and TP formation. The error bars represent the standard deviation (n = 3). (B) Proposed biotransformation pathways for **Cl-E1**. Unstable transient intermediates are shown in brackets. The thickness of the arrows represents the relative proportion of parent compound undergoing the different pathways. (C – D) Parent compound decay of **Cl-E2**, F^- and TP formation. TP188_Cl-E2 and TP128_Cl-E2 were quantified using reference standards and are shown on the right y-axis. (E) Proposed biotransformation pathways of **Cl-E2**. All TPs with designated names were detected. Transient intermediates are shown in brackets. The concentration of removed **Cl-E2** and specific TPs is shown in paratheses, where "c.a." indicates that the concentration was calculated based on the quantification of F^- and the TPs with reference standards (i.e., TP188 and TP128).

The major TP (TP496_Cl-E1) of **Cl-E1** (see **Figure S4** for the chromatogram and MS^1/MS^2 spectra for TPs of **Cl-E1**) was from reductive dechlorination (Cl → H) (**Figure 1B**). In a minor pathway, the terminal C–Cl bond underwent hydrolytic dechlorination, with Cl being replaced with a hydroxyl group (–OH). The formed fluoroalcohol intermediate was unstable and subject to spontaneous HF elimination and hydrolysis, forming an ether diacid, TP490_Cl-E1 (**Figure S4B**) as the minor TP. Only this hydrolytic dechlorination pathway led to two F^- release per one molecule of **Cl-E1** transformed. Given a total F^- formation of 17 μM by Day 128, the portion of **Cl-E1** underwent this defluorinating pathway was 8.5 μM. Thus, the remaining 37.5 μM out of the total removed **Cl-E1** (46 μM) underwent the non-defluorinating reductive dechlorination pathway. The same two pathways were also observed for Cl-terminal PFCAs.[41] The presence of an ether group in **Cl-E1** at the β-carbon, which is away from the Cl substitution,

260 did not affect the biotransformation pathways, as both occurred at the terminal position. In
261 addition, it is worth noting that the shorter RT of the two TPs (7.15 min and 5.87 min, compared
262 to 7.59 min for **Cl-E1**) suggests higher mobility than **Cl-E1**. The TPs tend to be released into
263 water bodies once formed from **Cl-E1** in anaerobic environments (e.g., soil and sediments). The
264 higher mobility and unknown toxicities of those fluorinated TPs may cause additional
265 environmental concerns and underscore the need for the risk assessment of derived PFAS from
266 environmental transformation in addition to the parent PFAS.

267 **Cl-E2**, which has an additional Cl substitution at the adjacent carbon, exhibited three
268 times higher total defluorination (7%) than the monochlorinated **Cl-E1**. Besides the reductive
269 (hydrogenolysis, forming TP326_Cl-E2) and hydrolytic dechlorination (forming TP128_Cl-E2,
270 TP188_Cl-E2, and TP286_Cl-E2 from TP326_Cl-E2) (see **Figure S5** for the chromatograph and
271 MS^1/MS^2 spectra of the identified TPs of **Cl-E2**), the two adjacent Cl substitutions of **Cl-E2**
272 enabled another type of reductive dechlorination, i.e., dichloroelimination,[46] which was another
273 pathway leading to additional fluoride release (**Figure 1E**). The fluorovinyl ether moiety
274 (CF_2=CF–O–) in TP290_Cl-E2, which was formed from dichloroelimination tends to be more
275 amenable to microbes. It facilitated the hydrolytic O-dealkylation, forming perfluorosuccinic
276 acid (TP188_Cl-E2 in **Figure 1E**) via spontaneous defluorination of the unstable fluoroalcohol
277 intermediate. It was structurally confirmed using the reference standard as shown in **Figure S5F**.
278 The hydrolytic O-dealkylation at a (fluoro)vinyl ether moiety (C=C–O–) was also observed in
279 aerobic conditions,[37, 47] suggesting the involvement of certain hydrolases that are non-oxygen-
280 sensitive, and no oxygen is needed for this hydrolysis reaction. The fluorovinyl ether moiety also
281 promoted the reductive defluorination at the C=C bond, forming TP272_Cl-E2 (**Figure 1E**,
282 **Figure S5E**). Here, the role of the ether group was similar to the carboxyl group in the reductive

defluorination of unsaturated per- and polyfluorocarboxylic acids.[48] It implies that the proximity to electron-withdrawing groups, like ether and carboxyl groups, could promote reductive defluorination at the C=C bond of unsaturated PFAS. TP272_Cl-E2 could be further transformed via hydrolytic O-dealkylation followed by spontaneous defluorination, forming TP188_Cl-E2 (**Figure 1E**).

The portion of **Cl-E2** undergoing each of the above-identified biotransformation pathway was further calculated based on the quantification of parent compound removal, fluoride formation, and the structurally confirmed TPs (i.e., TP128_Cl-E2 and TP188_Cl-E2). About 0.5 μM TP128_Cl-E2 was formed at the end (**Figure 1C**). This corresponded to 0.5 μM of TP188_Cl-E2 produced via the hydrolytic dechlorination pathway of **Cl-E2**. Given the total formation of ~ 2.5 μM TP188_Cl-E2, the remaining 2.0 μM was formed via the pathways initiated by the eliminative or reductive (F→H) dehalogenation forming TP 272_Cl-E2 as the intermediate (**Figure 1E**). Theoretically, five moles of F^- could be released per mole of TP188_Cl-E2 formed. The formed TP188_Cl-E2 (~ 2.5 μM) then corresponds to ~12.5 μM F^- from ~ 2.5 μM **Cl-E2** reacted. The remaining F^- (~ 20 μM) could then be attributed to the other defluorinating route initiated by the hydrogenolytic reductive dechlorination followed by hydrolytic dechlorination, resulting in TP286_Cl-E2 (**Figure 1E**). If the remaining 20 μM F^- was all from this route, it would correspond to 10 μM **Cl-E2** reacted. Thus, **Cl-E2** undergoing defluorinating pathways was 12.5 μM, while the remaining reacted **Cl-E2** (~40.5 μM) was subject to the non-defluorinating reductive dechlorination pathway, forming the two stable end products TP326(1)(2)_Cl-E2 and TP292_Cl-E2 (**Figure 1E**).

306 **Anaerobic biotransformation and defluorination of unsaturated ether PFAS**

307 All three unsaturated ether PFAS (**E1 – 3**) possess a fluorovinyl ether moiety, the same as that in
308 the dichloroelimination product of **Cl-E2** (TP290_Cl-E2). They exhibited great biodegradability
309 with substantial defluorination under anaerobic conditions. **E1** was defluorinated in both
310 biologically active and heat-inactivated samples in the anaerobic condition (**Figure S6A**), but
311 biological samples resulted in more parent compound decay and higher defluorination compared
312 to the abiotic controls (150 μM vs 81 μM F^- release). No transformation was observed under
313 aerobic conditions (**Figure S6B**), suggesting the transformation under anaerobic conditions
314 might require oxygen-sensitive reducing molecules. **E1** was likely transformed through reductive
315 defluorination and hydrolytic O-dealkylation pathways,[37, 49] but no respective TPs were detected,
316 leaving the transformation pathway elusive. Given the unsaturated and branched structure of **E1**,
317 similar to observations for other unsaturated and branched PFAS structures,[49] neutral
318 fluoroalkanes might be formed, which were not ionizable and thus undetectable by LC-
319 HRMS/MS.

320 For NBP1 and its analogue (**E2** and **E3**), hydrolytic O-dealkylation at the fluorovinyl
321 ether moiety was one of the major biotransformation pathways (**Figure 2** and **3**), forming
322 TP340_E2 and TP174_E3 (**Figure S7**), respectively. TP174_E3 was structurally confirmed using
323 the reference standard. This is consistent with the hydrolytic O-dealkylation for the eliminative
324 dechlorination product of **Cl-E2** (TP290_Cl-E2), which also contained the fluorovinyl ether
325 moiety. This reaction seemed not to be affected by the different head groups (i.e., sulfonic acid
326 vs. carboxylic acid). For **E2** with two ether bonds, the hydrolytic O-dealkylation was also likely
327 to occur at the other ether bond next to the $–CF_3$ branch (**Figure 2C**), forming the small end
328 product (TP174_E2). The slow formation of TP174_E2 and its low level suggest it a less

329 favorable pathway than the hydrolytic O-dealkylation at the fluorovinyl ether moiety. The
330 hydrolytic O-dealkylation of **E3** substantially decreased after one week, resulting in incomplete
331 transformation of **E3** (**Figure 3A**). This could be due to the toxicity of the small end product
332 TP174_E3, which was formed at a much higher level (~ 26 μM on day 7) than from **E2** (~ 0.23
333 μM). The hydrolytic O-dealkylation at the fluorovinyl ether moiety of **E2** and **E3** also occurred
334 under aerobic conditions, indicating the insensitivity of oxygen of this enzymatic reaction
335 (**Figure S9A & B**).

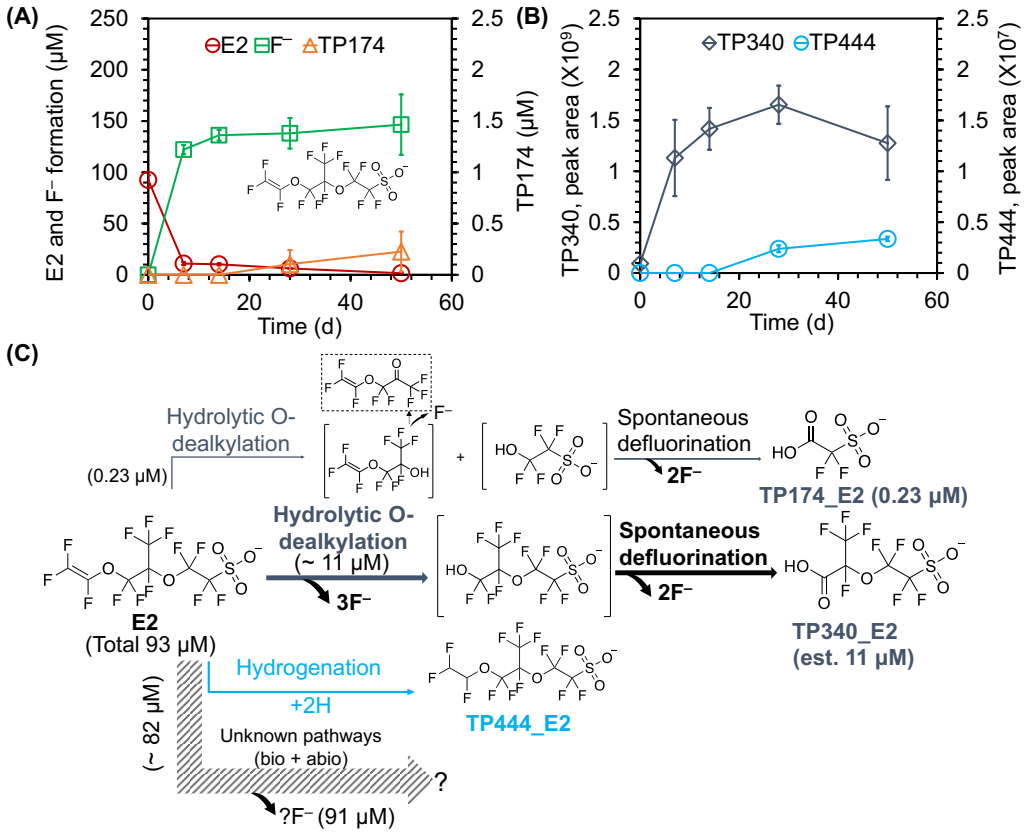

336

337 **Figure 2.** Biotransformation and defluorination of **E2** under anaerobic conditions. (A) Parent
338 compound decay of **E2**, F^- formation, and TP174. (B) Formation trend of TP340 and TP444. The
339 error bars represent the standard deviation (n = 3). (C) Proposed biotransformation pathways of
340 **E2**. All listed TPs were detected, except for those in dashed boxes and brackets. In dashed boxes

are the proposed TPs not detected by LC-HRMS/MS. In brackets are unstable transient intermediates. The concentration of removed **E2** and specific TPs is shown in paratheses, where "est." indicates that the concentration of TP340 was estimated based on F^- formation from aerobic transformation of **E2** via hydrolytic O-dealkylation and assuming it was the only defluorinating route in aerobic conditions. The thickness of arrows represents the approximate proportion of **E2** undergoing each pathway.

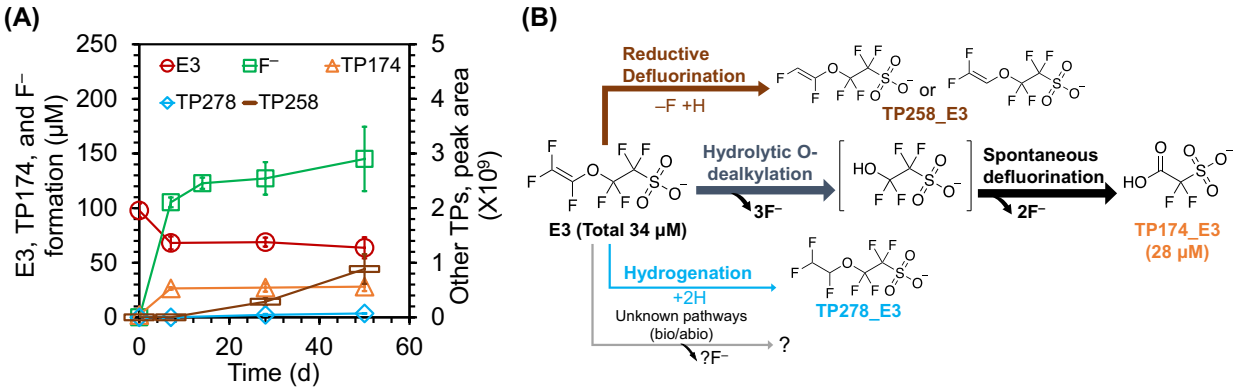

Figure 3. Biotransformation and defluorination of **E3** under anaerobic conditions. (A) Parent compound decay of **E3**, F^- and TP formation. The error bars represent the standard deviation (n = 3). (B) Proposed biotransformation pathways of **E3**. All listed TPs were detected, except for those in brackets, which are unstable transient intermediates. In parentheses is the calculated amount reacted or formed based on F^- measurements and LC-HRMS/MS results. The thickness of arrows suggests the estimated relative proportion of **E3** undergoing each pathway.

Besides the hydrolytic O-dealkylation, two other pathways were identified in anaerobic conditions. The TP of reductive defluorination in anaerobic conditions was detected for **E3** (TP258_E3, **Figure 3A** and **Figure S8**). However, it was not detected for **E2**, probably due to the longer and branched structure next to the fluorovinyl ether in **E2**, which caused a steric

360 hinderance of the enzyme binding. Additionally, hydrogenation of the C=C bond in E2 and E3
361 represented a minor anaerobic pathway, forming the hydrogenation products (TP444_E2 and
362 TP278_E3). Interestingly, in the abiotic controls under the anaerobic condition, **E2** and **E3**
363 exhibited substantial removal and a considerable amount of fluoride formation but at much
364 slower rates than the biological samples (**Figure S10**). However, no TPs identified from the three
365 biotransformation pathways (i.e., hydrolytic O-dealkylation, reductive defluorination, and
366 hydrogenation) were detected in those abiotic controls. It indicates that (i) the three pathways
367 were microbially mediated contributing to the rapid defluorination of the parent compound; (ii)
368 there were unknown abiotic defluorination pathways for **E2** and **E3**, which could only occur in
369 anaerobic but not aerobic conditions (**Figure S9B & D**).
370 We also performed a semi-quantitative calculation on how much **E2** and **E3** underwent
371 each pathway. We assumed that all fluoride formed in the aerobic biotransformation of **E2**
372 (**Figure S9A**) was from the hydrolytic O-dealkylation pathway, then every five F^- ions released
373 would correspond to one molecule of TP340_E2 formed. Based on the total fluoride formation
374 from **E2** under aerobic conditions at the end (~ 14 μM), there would be a maximum of 2.8 μM
375 TP340_E2 formed. The concentration of TP340_E2 was supposed to be proportional to the peak
376 area. Thus, the TP340_E2 formed in the anaerobic condition could be estimated to be 11 μM at
377 the maximum, which corresponds to a total of 55 μM F^- formation (**Figure 2C**). The other
378 hydrolytic O-dealkylation pathway forming 0.23 μM TP174_E2 contributed to less than 1 μM F^-
379 formation (3F^- per TP174_E2, **Figure 2C**). Given the total of 147 μM F^- formation from **E2**, the
380 remaining ~ 91 μM F^- could be attributed to unknown biological and abiotic pathways.
381 Moreover, since the abiotic transformation and defluorination was much slower, it unlikely
382 contributed to the rapid removal of ~ 82 μM **E2** and F^- formation within 7 days. Instead, this

383 majority of **E2** underwent some unidentified biodefluorinating pathways, with another 11 μM **E2**
384 undergoing the hydrolytic O-dealkylation pathway (**Figure 2C**). In comparison, the hydrolytic
385 O-dealkylation pathway was the dominant biotransformation pathway for **E3**. Among the 34 μM
386 reacted **E3**, over 80% underwent this route forming 28 μM the corresponding TP174_E3 within a
387 week, while other pathways, such as reductive defluorination, hydrogenation, and abiotic
388 defluorination, occurred more slowly over the time course of ~ 50 days (**Figure 3A** & **B**).
389

390 **Cobalt-enzyme-dependent anaerobes played a crucial role in the transformation of**
391 **chlorinated ether PFAS**

392 Enzymes known to catalyze hydrogenolytic reductive dechlorination (Cl→H) and
393 dichloroelimination (–2Cl) are usually those using corrinoids (cobalt-containing complexes) as
394 essential cofactors.[46, 50, 51] Thus, we hypothesized that cobalt (Co) enzymes are involved in the
395 reductive and eliminative dechlorinating reactions of chlorinated ether PFAS, but not in the
396 transformation of unsaturated ether PFAS, which mainly involves hydrolytic O-dealkylation. To
397 test this hypothesis, we compared biotransformation of chlorinated ether PFAS (**Cl-E2** as a
398 representative) and unsaturated ether PFAS (**E2** as a representative) in the anaerobic community
399 with and without the addition of Co species, i.e., the free cobalt ion (Co^{2+}) and the Co-complex
400 vitamin B_{12} (a corrinoid form with Co as the metal center). When Co was not provided, the
401 biotransformation of **Cl-E2**, regarding the parent compound removal and F^- and TP formation,
402 was nearly completely inhibited, whereas **E2** biotransformation remained unaffected compared
403 to the Co-added control (**Figure 4**). This result demonstrates that Co-enzyme-dependent
404 microbes played a major role in the first-step transformation of **Cl-E2** via the different
405 dechlorination reactions. It could be certain Co enzymes that directly catalyzed **Cl-E2**

406 dechlorination. Or, given that some Co enzymes are required in essential metabolic processes

407 (e.g., methionine synthesis) by certain microbes,[52, 53] Co deficiency could result in a cease of

408 microbial growth and activities in general, including **Cl-E2** biotransformation that was carried

409 out by those microbes but may or may not be catalyzed by Co enzymes.

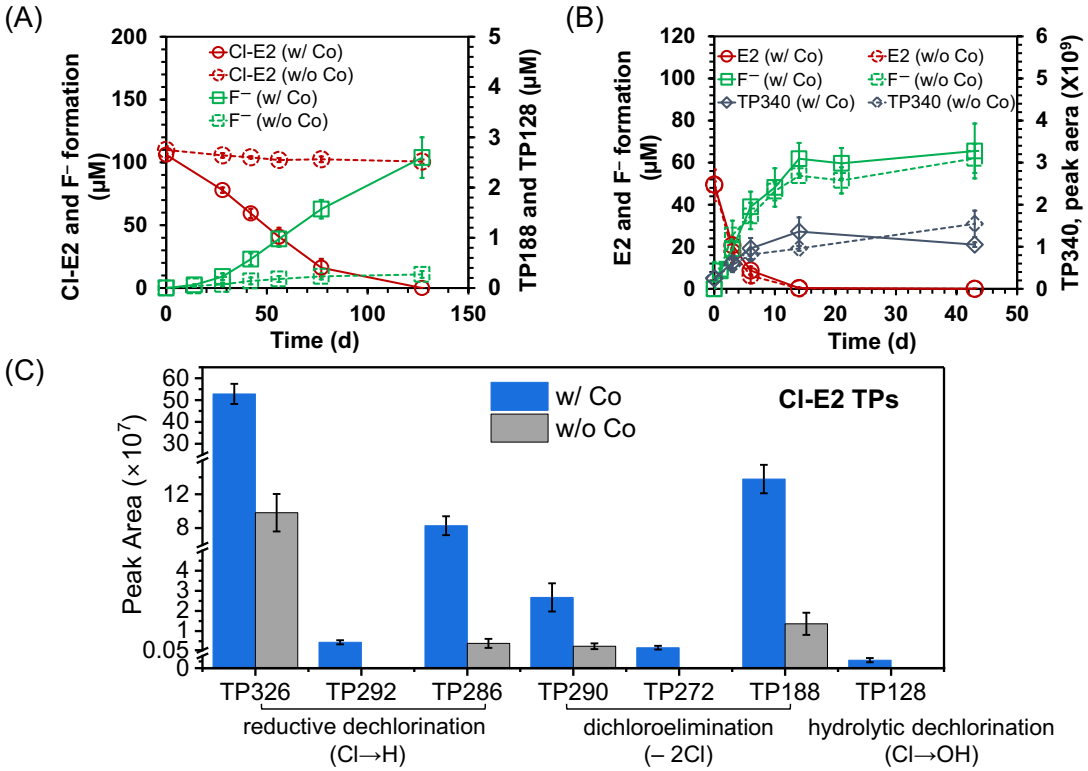

410

411 **Figure 4.** Biotransformation of **Cl-E2** and **E2** in the anaerobic microbial community with and

412 without the addition of Co in the forms of Co^{2+} and B_{12}. (A: **Cl-E2** decay and fluoride formation;

413 B: **E2** decay and fluoride formation; C: formation of **Cl-E2** TPs, TPs are grouped by the primary

414 transformation reaction that led to their formation, i.e., reductive dechlorination (Cl → H),

415 dichloroelimination (– 2Cl), and hydrolytic dechlorination (Cl → OH); n= 3, error bars represent

416 the standard deviation)

417

418 In contrast, **E2** can be transformed by quite different microbial groups that are
419 independent of Co enzymes. One major biotransformation pathway of **E2** was hydrolytic O-
420 dealkylation forming TP340_E2 (**Figure 2C** and **Figure 4B**), which is likely catalyzed by less
421 specific enzymes possessed by a broader spectrum of microbes. As the unsaturated TP290_Cl-E2
422 formed from dichloroelimination of **Cl-E2** is structurally similar to **E2**, its further
423 biotransformation in the anaerobic community likely involved the same microbial groups for **E2**
424 biotransformation. Thus, **Cl-E2** biotransformation may involve cooperative action among
425 different microbial groups, with Co-enzyme-dependent microbes catalyzing the primary
426 dechlorination reactions, followed by other microbes degrading the resulting unsaturated
427 intermediates.
428
429 **Specific microbial groups involved in Cl-E2 and E2 biotransformation**
430 One group of Co-enzyme-dependent anaerobes is methanogens, which utilize corrinoid-
431 dependent methyltransferases in methanogenesis. How methanogens contributed to **Cl-E2**
432 biotransformation was investigated using an inhibition experiment, where methanogenesis was
433 inhibited by 2-bromoethanesulfonate (BES), a structural analogue of coenzyme M that
434 specifically inhibits methanogenesis. When methanogenesis was inhibited, **Cl-E2** removal
435 decreased by 49% together with a 52 – 69% decrease in the formation of primary TPs from the
436 reductive (TP326) and eliminative (TP290) dechlorination routes, as well as the downstream end
437 products TP286 and TP188 (**Figure S11**). This indicates that methanogens were one significant
438 but not the only contributor to the primary transformation of **Cl-E2**. Other Co-enzyme-dependent
439 bacteria may also play a role.

440 We previously identified two anaerobic bacteria in an anaerobic microbial community
441 originating from the same source of activated sludge, i.e., *Sporomusa sphaeroides* and
442 *Desulfovibrio aminophilus*,[41] which were able to transform chlorotrifluoroethylene (CTFE)
443 oligomer acids. Based on the genomic analysis, *S. spharoides* has the B_{12}-dependent methionine
444 synthase (MetH), and thus is Co-enzyme dependent, while *D. aminophilus* has the B_{12}-
445 independent methionine synthase (MetE) and could be independent of Co-enzymes in central
446 metabolism. Thus, we compared biotransformation activities of both bacteria for **Cl-E2** and **E2**
447 to examine their roles in the different pathways. Interestingly, the two bacteria exhibited distinct
448 transformation activities for **Cl-E2** and **E2**. *S. sphaeroides* was able to transform 80% of the
449 initial ~ 50 μM **Cl-E2** over 100 days with 80 μM F^- formation (avg. ~ 2F per **Cl-E2**
450 transformed) and the formation of TPs involved in the reductive and eliminative dechlorination
451 pathways (i.e., TP326, TP292, TP290, TP286, and TP188) (**Figure 5A&B**). In comparison, *D.*
452 *aminophilus* only exhibited minimal **Cl-E2** removal (12%) and a slight formation of F^- (9 μM)
453 with no substantial formation of TPs except for the first reductive dechlorination product TP326
454 (**Figure 5A&B**). The absence of TP290_Cl-E2 in *D. aminophilus* indicates a possible lack of
455 enzymes necessary for eliminative dechlorination. This is consistent with the transformation of
456 CTFE oligomer acids by *D. aminophilus*, where little eliminative dechlorination TPs were
457 formed.[41] However, *D. aminophilus* showed substantial defluorination of CTFE dimer acid also
458 with two Cl substitutions via hydrolytic dechlorination. This emphasizes the structural specificity
459 of biotransformation, and ether groups in **Cl-E2** might alter its biodegradability in *D.*
460 *aminophilus*. Notably, the total defluorination of **Cl-E2** was three times higher in *S. sphaeroides*
461 than in the anaerobic mixed culture (23.3% vs. 6.9%) (**Figure 5A** and **Figure 1C**), despite the
462 lower cell density than the mixed culture (**Figure S12**). It could be attributed to the higher

463 formation of the defluorinating end products, TP188, TP128, and TP286 (**Figure 5B** and **Figure**
464 **1D**). This result also corroborates findings from the Co limitation and BES inhibition
465 experiments that Co-enzyme-dependent microbes played a crucial role in chlorinated ether PFAS
466 biotransformation.

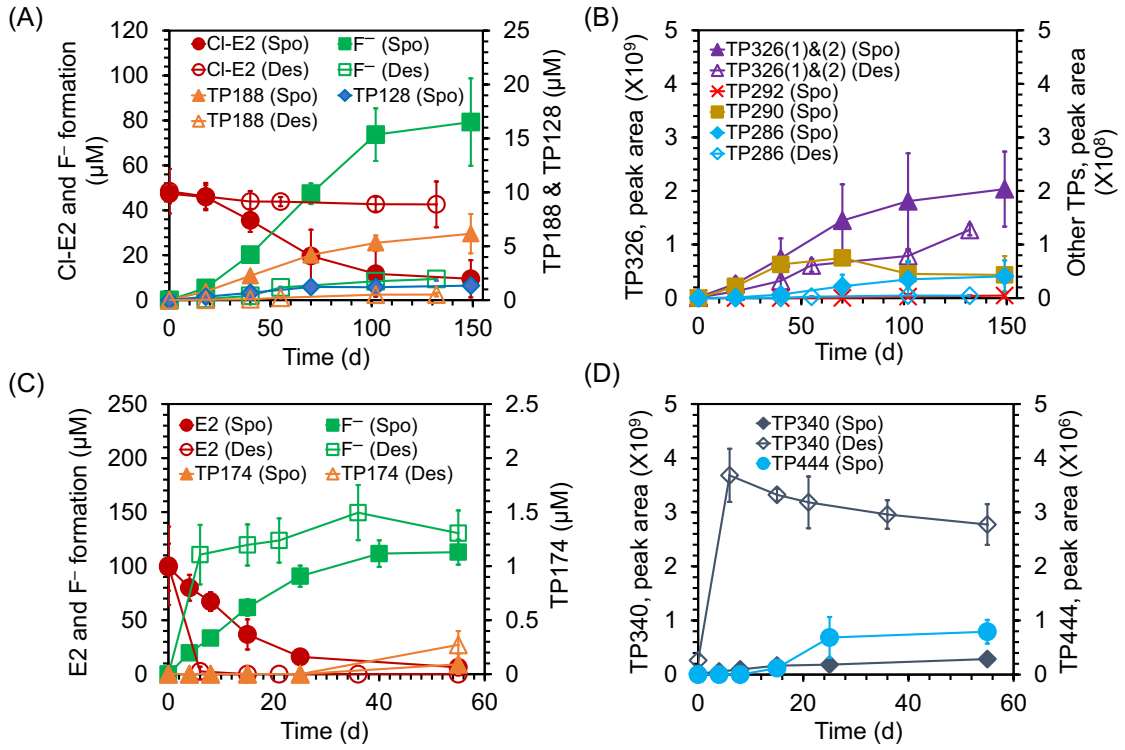

467

468 **Figure 5.** Anaerobic biotransformation of **Cl-E2** (**A – B**) and **E2** (**C – D**) by *Sporomusa*
469 *sphaeroides* (Spo) and *Desulfovibrio aminophilus* (Des) (error bars represent standard deviation,
470 n=3).

471

472 On the other hand, as for the unsaturated ether **E2**, both bacteria showed complete parent
473 compound transformation and similar total defluorination (9 – 10%), with *D. aminophilus* having
474 a faster **E2** removal and fluoride formation than *S. sphaeroides* (**Figure 5C&D**). **E2** was
475 depleted in *D. aminophilus* within a week, while it took more than 25 days for *S. sphaeroides*.
476 This could be due to the higher optimal growth of *D. aminophilus* than *S. sphaeroides* (**Figure**

477 **S12**). More interestingly, much higher levels of TP340_E2 and TP174_E2, the two TPs from the
478 hydrolytic O-dealkylation pathway, were formed in *D. aminophilus*, while the hydrogenation
479 product of **E2** was only detected in *S. sphaeroides*. TP340_E2 was formed 2 – 3 times higher in
480 *D. aminophilus* than in the anaerobic mixed culture (**Figure 2B**), corresponding to 22 – 33 μM in
481 *D. aminophilus* based on the semi-quantification of TP340_E2 in the mixed culture (**Figure 2C**).
482 As five F^- could be released per TP340_E2 molecule formed, all F^- detected in *D. aminophilus*
483 (130 – 150 μM) could be attributed to this hydrolytic O-dealkylation pathway. The hydrolytic O-
484 dealkylation route forming TP174 (0.27 μM) again only contributed to less than 1 μM F^-
485 formation like in the mixed culture. The rest of the removed **E2** (~ 70 – 80 μM) by *D.*
486 *aminophilus* likely underwent non-defluorinating pathways, which remained elusive. Given the
487 ten times lower formation of TP340_E2 and the similar total F^- formation in *S. sphaeroides*
488 compared to *D. aminophilus* (**Figure 5C&D**), *S. sphaeroides* might carry out other unknown
489 defluorinating pathways as those implied in the mixed culture (**Figure 2C**).
490 Collectively, Co-enzyme-dependent microbes, such as methanogens and *S. sphaeroides*,
491 made a major contribution to the biotransformation of chlorinated ether PFAS like **Cl-E2** by
492 carrying out the primary transformation via dechlorination reactions, especially reductive and
493 eliminative dechlorination. They may also be able to continue to transform the unsaturated
494 intermediate formed from eliminative dechlorination, but given the slow kinetics their
495 contribution to the transformation of unsaturated ether PFAS was insignificant. Instead, Co-
496 enzyme-independent sulfate-reducing bacteria such as *D. aminophilus* excelled in rapidly
497 transforming unsaturated ether PFAS like **E2** via the hydrolytic O-dealkylation pathway.
498
499 **Environmental Implications**

500 Given the use of ether PFAS in some essential applications and their widespread environmental
501 occurrence, this study provides critical insights into their environmental fate, especially for the
502 fully halogenated structures. First, biodegradability and biotransformation pathways are
503 structure-specific, meaning that the presence of certain functional moieties enables distinct
504 biological reactions. Also, the observed defluorination of the investigated ether PFAS was mostly
505 triggered by primary reactions occurring at non-C–F bonds. For example, fully halogenated ether
506 PFAS (with Cl- and F-substitutions) first underwent dechlorination reactions exclusively in
507 anaerobic conditions. Intermediates formed from hydrolytic and eliminative dechlorination could
508 further undergo spontaneous or biological defluorination. Increased biodegradability was
509 associated with a greater degree of Cl substitution, consistent with our previous findings for
510 other chlorinated PFAS without ether groups.[41] Unsaturated fully fluorinated ether PFAS with
511 fluorovinyl ether moieties, such as NBP1 and analogues, may undergo rapid biotransformation in
512 both anaerobic and aerobic conditions via hydrolytic O-dealkylation. Anaerobic conditions
513 resulted in higher total defluorination, likely due to the involvement of additional anaerobic
514 defluorination pathways beyond hydrolytic O-dealkylation. Despite the presence of more
515 microbially amenable moieties, the investigated chlorinated and unsaturated ether PFAS were
516 still not completely defluorinated, leading to some signature end TPs such as shorter chain diacid
517 (ether) PFAS and H-substituted ether PFAS, which could be used for PFAS source-tracking and
518 suggest potential PFAS exposure profiles in the environment.

519 Second and more importantly, we demonstrate microbes involved in different structure-
520 specific biotransformation reactions. Specifically, co-enzyme-dependent anaerobes, including
521 methanogens and *Sporomusa* spp., played a crucial role in the primary dechlorination of
522 chlorinated ether PFAS, while the biotransformation of unsaturated ether PFAS was mainly

carried out by microbes independent of Co-enzymes, such as certain sulfate-reducing bacteria. It highlights that the environmental biotransformation of certain PFAS structures could be a result of multiple reactions in series collaboratively achieved by different microbes in a community. Thus, PFAS biotransformation could be tuned by having the desired microbes in a defined consortium to promote transformation routes that lead to higher defluorination and less toxic products. It is worth noting that the observed PFAS biotransformation was cometabolic. As a result, transformation rates are biomass-dependent. The occurrence and kinetics of the identified biotransformation pathways in other environmental settings will depend on microbial community composition, as well as the abundance and activity of the responsible taxa.

Overall, this study fills the knowledge gap of the environmental fate and biotransformation of commonly used ether PFAS and advances the fundamental knowledge of the responsible microbial groups and how they work together in different transformation pathways. These findings provide important guidance for PFAS exposure and risk assessment, as well as environmental source tracking. It also sheds light on the development of cost-effective treatment systems involving biological processes by defined consortia and the design of more environmentally biodegradable alternative PFAS.

Acknowledgements

We would like to acknowledge staff from the Western Riverside County Regional Wastewater Authority for providing the activated sludge samples. This study was supported by the Strategic Environmental Research and Development Program (project No. ER20-1541, for B.J., Y.Y., Y.M., Z.L., and J.L.) and the National Institute of Environmental Health Sciences (award No. R01ES032668 for S.C., W.Z., and Y.M.).

Reference

1. Evich, M. G.; Davis, M. J. B.; McCord, J. P.; Acrey, B.; Awkerman, J. A.; Knappe, D. R. U.; Lindstrom, A. B.; Speth, T. F.; Tebes-Stevens, C.; Strynar, M. J.; Wang, Z.; Weber, E. J.; Henderson, W. M.; Washington, J. W. Per- and polyfluoroalkyl substances in the environment. *Science* **2022,** *375*, (6580).

2. Wackett, L. P. Why Is the Biodegradation of Polyfluorinated Compounds So Rare? *mSphere* **2021,** *6*, (5), 10.1128/msphere.00721-00721.

3. Dickman, R. A.; Aga, D. S. A review of recent studies on toxicity, sequestration, and degradation of per- and polyfluoroalkyl substances (PFAS). *J. Hazard. Mater.* **2022,** *436*, 129120.

4. Jin, B.; Mallula, S.; Golovko, S. A.; Golovko, M. Y.; Xiao, F. In Vivo Generation of PFOA, PFOS, and Other Compounds from Cationic and Zwitterionic Per- and Polyfluoroalkyl Substances in a Terrestrial Invertebrate (Lumbricus terrestris). *Environ. Sci. Technol.* **2020,** *54*, (12), 7378-7387.

5. Cao, H.; Peng, J.; Zhou, Z.; Yang, Z.; Wang, L.; Sun, Y.; Wang, Y.; Liang, Y. Investigation of the Binding Fraction of PFAS in Human Plasma and Underlying Mechanisms Based on Machine Learning and Molecular Dynamics Simulation. *Environ. Sci. Technol.* **2023,** *57*, (46), 17762-17773.

6. Adu, O.; Ma, X.; Sharma, V. K. Bioavailability, phytotoxicity and plant uptake of per-and polyfluoroalkyl substances (PFAS): A review. *J. Hazard. Mater.* **2023,** *447*, 130805.

7. Pickard, H. M.; Ruyle, B. J.; Thackray, C. P.; Chovancova, A.; Dassuncao, C.; Becanova, J.; Vojta, S.; Lohmann, R.; Sunderland, E. M. PFAS and Precursor Bioaccumulation in

569 Freshwater Recreational Fish: Implications for Fish Advisories. *Environ. Sci. Technol.* **2022,** *56*,
570 (22), 15573-15583.
571 8. Qian, S.; Lu, H.; Xiong, T.; Zhi, Y.; Munoz, G.; Zhang, C.; Li, Z.; Liu, C.; Li, W.; Wang,
572 X.; He, Q. Bioaccumulation of Per- and Polyfluoroalkyl Substances (PFAS) in Ferns: Effect of
573 PFAS Molecular Structure and Plant Root Characteristics. *Environ. Sci. Technol.* **2023,** *57*, (11),
574 4443-4453.
575 9. Biden-Harris Administration Finalizes First-Ever National Drinking Water Standard to
576 Protect 100M People from PFAS Pollution. https://www.epa.gov/newsreleases/biden-harris-
577 administration-finalizes-first-ever-national-drinking-water-
578 standard#:~:text=EPA%20is%20setting%20enforceable%20Maximum,%2C%20and%20%E2%8
579 0%9CGenX%20Chemicals.%E2%80%9D
580 10. Sun, M.; Arevalo, E.; Strynar, M.; Lindstrom, A.; Richardson, M.; Kearns, B.; Pickett, A.;
581 Smith, C.; Knappe, D. R. U. Legacy and Emerging Perfluoroalkyl Substances Are Important
582 Drinking Water Contaminants in the Cape Fear River Watershed of North Carolina. *Environ. Sci.*
583 *Technol. Lett.* **2016,** *3*, (12), 415-419.
584 11. Hopkins, Z. R.; Sun, M.; DeWitt, J. C.; Knappe, D. R. U. Recently Detected Drinking
585 Water Contaminants: GenX and Other Per- and Polyfluoroalkyl Ether Acids. *J. Am. Water Works*
586 *Assoc.* **2018,** *110*, (7), 13-28.
587 12. Munoz, G.; Liu, J.; Duy, S. V.; Sauvé, S. Analysis of F-53B, Gen-X, ADONA, and
588 emerging fluoroalkylether substances in environmental and biomonitoring samples: A review.
589 *Trends Environ. Anal. Chem.* **2019,** *23*, e00066.

590 13. Hamid, N.; Junaid, M.; Sultan, M.; Yoganandham, S. T.; Chuan, O. M. The untold story
591 of PFAS alternatives: Insights into the occurrence, ecotoxicological impacts, and removal
592 strategies in the aquatic environment. *Water Res.* **2024,** *250*, 121044.
593 14. Ruan, T.; Lin, Y. F.; Wang, T.; Liu, R. Z.; Jiang, G. B. Identification of Novel
594 Polyfluorinated Ether Sulfonates as PFOS Alternatives in Municipal Sewage Sludge in China.
595 *Environ. Sci. Technol.* **2015,** *49*, (11), 6519-6527.
596 15. Bao, Y. X.; Qu, Y. X.; Huang, J.; Cagnetta, G.; Yu, G.; Weber, R. First assessment on
597 degradability of sodium p-perfluorous nonenoxybenzene sulfonate (OBS), a high volume
598 alternative to perfluorooctane sulfonate in fire-fighting foams and oil production agents in China.
599 *Rsc Adv.* **2017,** *7*, (74), 46948-46957.
600 16. Xu, L.; Shi, Y.; Li, C.; Song, X.; Qin, Z.; Cao, D.; Cai, Y. Discovery of a Novel
601 Polyfluoroalkyl Benzenesulfonic Acid around Oilfields in Northern China. *Environ. Sci. Technol.*
602 **2017**.
603 17. Cousins, I. T.; Goldenman, G.; Herzke, D.; Lohmann, R.; Miller, M.; Ng, C. A.; Patton,
604 S.; Scheringer, M.; Trier, X.; Vierke, L.; Wang, Z.; DeWitt, J. C. The concept of essential use for
605 determining when uses of PFASs can be phased out. *Environ. Sci. Process. Impacts.* **2019,** *21*,
606 (11), 1803-1815.
607 18. Li, Y.; Wen, Q.; Zou, S.; Dan, X.; Ning, F.; Li, W.; Xu, P.; He, C.; Shen, M.; He, L.; Tian,
608 B.; Zhou, X. Multiscale Architectured Nafion Membrane Derived from Lotus Leaf for Fuel Cell
609 Applications. *ACS Appl. Mater. Interfaces* **2023,** *15*, (24), 29084-29093.
610 19. Prykhodko, Y.; Fatyeyeva, K.; Hespel, L.; Marais, S. Progress in hybrid composite
611 Nafion®-based membranes for proton exchange fuel cell application. *Chem. Eng. J.* **2021,** *409*,
612 127329.

20. Zhi, Z.; Gao, W.; Yang, J.; Geng, C.; Yang, B.; Tian, C.; Fan, S.; Li, H.; Li, J.; Hua, Z. Amperometric hydrogen gas sensor based on Pt/C/Nafion electrode and ionic electrolyte. *Sens. Actuators B Chem.* **2022,** *367*, 132137.

21. Jeon, J.-Y.; Kang, B.-C.; Ha, T.-J. Flexible pH sensors based on printed nanocomposites of single-wall carbon nanotubes and Nafion. *Appl. Surf. Sci.* **2020,** *514*, 145956.

22. Rice, P. A.; Cooper, J.; Koh-Fallet, S. E.; Kabadi, S. V. Comparative analysis of the physicochemical, toxicokinetic, and toxicological properties of ether-PFAS. *Toxicol. Appl. Pharmacol.* **2021,** *422*, 115531.

23. Gebreab, K. Y.; Benetti, D.; Grosell, M.; Stieglitz, J. D.; Berry, J. P. Toxicity of perfluoroalkyl substances (PFAS) toward embryonic stages of mahi-mahi (Coryphaena hippurus). *Ecotoxicol.* **2022,** *31*, (7), 1057-1067.

24. Ge, Y.; Wang, Z.; Chen, X.; Wang, W.; Liu, Z.; Sun, H.; Zhang, L. Comparative toxicological effects of perfluorooctane sulfonate and its alternative 6:2 chlorinated polyfluorinated ether sulfonate on earthworms. *Environ. Toxicol. Chem.* **2024,** *43*, (1), 170-181.

25. Buck, R. C. Toxicology Data for Alternative "Short-Chain" Fluorinated Substances. In *Toxicological Effects of Perfluoroalkyl and Polyfluoroalkyl Substances*, DeWitt, J. C., Ed. Springer International Publishing: Cham, 2015; pp 451-477.

26. USEPA Human Health Toxicity Values for Hexafluoropropylene Oxide (HFPO) Dimer Acid and Its Ammonium Salt (In CASRN 13252-13-6 and CASRN 62037-80-3). 822R-21-010.: Washington, D.C., 2021.

27. Gui, W.; Guo, H.; Wang, J.; Wang, C.; Guo, Y.; Zhang, K.; Dai, J.; Zhao, Y. Nafion by-product 2 disturbs lipid homeostasis in zebrafish embryo. *Environ. Pollut.* **2023,** *322*, 121178.

28. Wang, Z.; Yao, J.; Guo, H.; Sheng, N.; Guo, Y.; Dai, J. Comparative Hepatotoxicity of a Novel Perfluoroalkyl Ether Sulfonic Acid, Nafion Byproduct 2 (H-PFMO2OSA), and Legacy Perfluorooctane Sulfonate (PFOS) in Adult Male Mice. *Environ. Sci. Technol.* **2022,** *56*, (14), 10183-10192.

29. Brunn, H.; Arnold, G.; Körner, W.; Rippen, G.; Steinhäuser, K. G.; Valentin, I. PFAS: forever chemicals—persistent, bioaccumulative and mobile. Reviewing the status and the need for their phase out and remediation of contaminated sites. *Environ. Sci. Eur.* **2023,** *35*, (1), 20.

30. Li, Y.; Yao, J.; Pan, Y.; Dai, J.; Tang, J. Trophic behaviors of PFOA and its alternatives perfluoroalkyl ether carboxylic acids (PFECAs) in a coastal food web. *J. Hazard. Mater.* **2023,** *452*, 131353.

31. Munoz, G.; Liu, J.; Duy, S. V.; Sauvé, S. Analysis of F-53B, Gen-X, ADONA, and emerging fluoroalkylether substances in environmental and biomonitoring samples: A review. *Tren. Environ. Anal. Chem.* **2019,** *23*, e00066.

32. Kirkwood-Donelson, K. I.; Dodds, J. N.; Schnetzer, A.; Hall, N.; Baker, E. S. Uncovering per- and polyfluoroalkyl substances (PFAS) with nontargeted ion mobility spectrometry-mass spectrometry analyses. *Sci. Adv.* **2023,** *9*, (43), eadj7048.

33. Petre, M. A.; Genereux, D. P.; Koropeckyj-Cox, L.; Knappe, D. R. U.; Duboscq, S.; Gilmore, T. E.; Hopkins, Z. R. Per- and Polyfluoroalkyl Substance (PFAS) Transport from Groundwater to Streams near a PFAS Manufacturing Facility in North Carolina, USA. *Environ. Sci. Technol.* **2021,** *55*, (9), 5848-5856.

34. Kotlarz, N.; Guillette, T.; Critchley, C.; Collier, D.; Lea, C. S.; McCord, J.; Strynar, M.; Cuffney, M.; Hopkins, Z. R.; Knappe, D. R. U.; Hoppin, J. A. Per- and polyfluoroalkyl ether

acids in well water and blood serum from private well users residing by a fluorochemical facility near Fayetteville, North Carolina. *J. Expo. Sci. Environ. Epidemiol.* **2024,** *34*, (1), 97-107.

35. Kirkwood, K. I.; Fleming, J.; Nguyen, H.; Reif, D. M.; Baker, E. S.; Belcher, S. M. Utilizing Pine Needles to Temporally and Spatially Profile Per- and Polyfluoroalkyl Substances (PFAS). *Environ. Sci. Technol.* **2022,** *56*, (6), 3441-3451.

36. Robuck, A. R.; Cantwell, M. G.; McCord, J. P.; Addison, L. M.; Pfohl, M.; Strynar, M. J.; McKinney, R.; Katz, D. R.; Wiley, D. N.; Lohmann, R. Legacy and Novel Per- and Polyfluoroalkyl Substances in Juvenile Seabirds from the U.S. Atlantic Coast. *Environ. Sci. Technol.* **2020,** *54*, (20), 12938-12948.

37. Jin, B.; Zhu, Y.; Zhao, W.; Liu, Z.; Che, S.; Chen, K.; Lin, Y. H.; Liu, J.; Men, Y. Aerobic Biotransformation and Defluorination of Fluoroalkylether Substances (ether PFAS): Substrate Specificity, Pathways, and Applications. *Environ. Sci. Technol. Lett.* **2023,** *10*, (9), 755-761.

38. Yi, S.; Zhu, L.; Mabury, S. A. First Report on In Vivo Pharmacokinetics and Biotransformation of Chlorinated Polyfluoroalkyl Ether Sulfonates in Rainbow Trout. *Environ. Sci. Technol.* **2020,** *54*, (1), 345-354.

39. Yi, S.; Morson, N.; Edwards, E. A.; Yang, D.; Liu, R.; Zhu, L.; Mabury, S. A. Anaerobic Microbial Dechlorination of 6:2 Chlorinated Polyfluorooctane Ether Sulfonate and the Underlying Mechanisms. *Environ. Sci. Technol.* **2022,** *56*, (2), 907-916.

40. Gao, J.; Liu, Z.; Chen, Z.; Rao, D.; Che, S.; Gu, C.; Men, Y.; Huang, J.; Liu, J. Photochemical degradation pathways and near-complete defluorination of chlorinated polyfluoroalkyl substances. *Nat. Water* **2023,** *1*, (4), 381-390.

41. Jin, B.; Liu, H.; Che, S.; Gao, J.; Yu, Y.; Liu, J.; Men, Y. Substantial defluorination of polychlorofluorocarboxylic acids triggered by anaerobic microbial hydrolytic dechlorination. *Nat. Water* **2023,** *1*, (5), 451-461.

42. Liu, H.; Wang, J.; Wang, A.; Chen, J. Chemical inhibitors of methanogenesis and putative applications. *Appl. Microbiol. Biotechnol.* **2011,** *89*, (5), 1333-1340.

43. Che, S.; Jin, B.; Liu, Z.; Yu, Y.; Liu, J.; Men, Y. Structure-Specific Aerobic Defluorination of Short-Chain Fluorinated Carboxylic Acids by Activated Sludge Communities. *Environ. Sci. Technol. Lett.* **2021,** *8*, (8), 668-674.

44. Schymanski, E. L.; Jeon, J.; Gulde, R.; Fenner, K.; Ruff, M.; Singer, H. P.; Hollender, J. Identifying small molecules via high resolution mass spectrometry: communicating confidence. *Environ. Sci. Technol.* **2014,** *48*, (4), 2097-2098.

45. Charbonnet, J. A.; McDonough, C. A.; Xiao, F.; Schwichtenberg, T.; Cao, D.; Kaserzon, S.; Thomas, K. V.; Dewapriya, P.; Place, B. J.; Schymanski, E. L. Communicating confidence of per-and polyfluoroalkyl substance identification via high-resolution mass spectrometry. *Environ. Sci. Technol. Lett.* **2022,** *9*, (6), 473-481.

46. Holliger, C.; Regeard, C.; Diekert, G. Dehalogenation by Anaerobic Bacteria. In *Dehalogenation: Microbial Processes and Environmental Applications*, Häggblom, M. M.; Bossert, I. D., Eds. Springer US: Boston, MA, 2003; pp 115-157.

47. White, G. F.; Russell, N. J.; Tidswell, E. C. Bacterial scission of ether bonds. *Microbiol. Rev.* **1996,** *60*, (1), 216-232.

48. Yu, Y.; Che, S.; Ren, C.; Jin, B.; Tian, Z.; Liu, J.; Men, Y. Microbial Defluorination of Unsaturated Per- and Polyfluorinated Carboxylic Acids under Anaerobic and Aerobic Conditions: A Structure Specificity Study. *Environ. Sci. Technol.* **2022,** *56*, (8), 4894-4904.

701 49. Yu, Y.; Zhang, K.; Li, Z.; Ren, C.; Chen, J.; Lin, Y. H.; Liu, J.; Men, Y. Microbial
702 Cleavage of C-F Bonds in Two C(6) Per- and Polyfluorinated Compounds via Reductive
703 Defluorination. *Environ. Sci. Technol.* **2020,** *54*, (22), 14393-14402.
704 50. Loffler, F. E.; Champine, J. E.; Ritalahti, K. M.; Sprague, S. J.; Tiedje, J. M. Complete
705 reductive dechlorination of 1,2-dichloropropane by anaerobic bacteria. *Appl. Environ. Microbiol.*
706 **1997,** *63*, (7), 2870-2875.
707 51. Padilla-Crespo, E.; Yan, J.; Swift, C.; Wagner Darlene, D.; Chourey, K.; Hettich Robert,
708 L.; Ritalahti Kirsti, M.; Löffler Frank, E. Identification and Environmental Distribution of dcpA,
709 Which Encodes the Reductive Dehalogenase Catalyzing the Dichloroelimination of 1,2-
710 Dichloropropane to Propene in Organohalide-Respiring Chloroflexi. *Appl. Environ. Microbiol.*
711 **2014,** *80*, (3), 808-818.
712 52. Roth, J. R.; Lawrence, J. G.; Bobik, T. A. Cobalamin (coenzyme B12): synthesis and
713 biological significance. *Annu. Rev. Microbiol.* **1996,** *50*, 137-181.
714 53. Banerjee, R.; Ragsdale, S. W. The many faces of vitamin B12: catalysis by cobalamin-
715 dependent enzymes. *Annu. Rev. Biochem.* **2003,** *72*, (1), 209-247.
716